

# Interaction between tunnels and slopes. Analysis of weak rock masses considering the Hoek-Brown failure criterion

Carlos Luis Garrido Garrido  
*AECOM, Enterprise Capabilities Europe*

Sergio Sánchez Rodríguez  
*AECOM, Enterprise Capabilities Europe*

Paula del Pozo García  
*AECOM, Enterprise Capabilities Europe*

**ABSTRACT:** Primary support design for tunnels close to a slope should consider the existing asymmetric stress state. Tunnel excavation imposes deconfinement around the cavity, which may affect the available margin of safety of the slope. For fair to good rock masses, the impact on the existing slope is mostly conditioned by the rock mass structure, even for shallow tunnels. This research is focused on analyzing the impact on the primary support needs for openings in weak rock masses, as well as the potential changes in the stability conditions of the slopes caused by shallow tunnels excavated near them. The Hoek-Brown failure criterion has been used for the parametric study carried out by means of numerical analysis. With these numerical simulations, the construction process of the tunnel is studied to analyze its influence on the existing slope stability, along with the corresponding effects on the support needs for different rock mass conditions.

*Keywords: Tunnel-slope interaction, slope stability, factor of safety, weak rock masses, Hoek-Brown failure criterion, numerical models.*

## 1 INTRODUCTION

Current status of tunnelling industry and technology have allowed mountain tunnels to be understood as a sum of activities which conform the excavation and support cycle. The adequate selection of the construction equipment and support systems have resulted in the successful completion of tens of tunnel kilometers in the last years. Of course, tunnelling works still have to deal with many challenges, such as complex tensional conditions, water-bearing rock masses, fault crossing, etc., which can lead to delays and extra costs. The risk of slope instability at tunnel portals is also one of those key issues, which also affects small or non-complex mountain tunnels.

A less frequent cause of delays and tunnel-slope interaction is the affection or re-activation of pre-existing landslides. This phenomenon has been less studied, but there are several practical cases that can provide an interesting number of lessons learnt. A compilation of these experiences is included in Sanchez & Garrido (2022) and comprises instabilities in the Italian Apennines, as well as some Spanish and Chinese cases. Pre-existing deep landslides with low displacement ratios, limited investigation during planning phases, and weak rock masses are the common factors of these

tunnelling experiences that, anyhow, could be handled with the current tunnelling investigation and design tools.

Therefore, when tunnels are built near natural slopes, their initial stability and tensional conditions are changed, causing or reactivating landslides that could also affect the tunnel safety. The closer the tunnel to the existing slope or instabilities, the greater the impacts on the environment and the tunnel itself. This paper is focused on the specific case of tunnels running in hilly terrain and crossing weak rocks, analyzing the impact on the tunnel design and the pre-existing slope stability conditions for rock masses where the Hoek-Brown failure criterion can be applied.

## 2 MAIN PARAMETERS CONDITIONING THE INTERACTION

Authors such as Wang (2010) and Koizumi et al. (2010) highlighted that the interaction between the tunnel and a sliding surface near it increases considerably below 1.5 to 2 diameters of distance ( $1.5D$ - $2D$ ). As a result, these distances are the minimum values that should be adopted to reduce or minimize any form of undesired impact on the pre-existing stability conditions or the design of the tunnel support. However, the distance from the tunnel is not the only factor to consider, being other factors that affect the interaction between tunnels and slopes that must be considered. These variables can result in increased distance requirements or additional support needs. Some of these relevant aspects are detailed below:

- Factor of safety of the slope prior to the tunnel execution.
- General ground conditions: height and gradient of the slope, geomechanical parameters of the rock mass, groundwater conditions, etc.
- Environmental and external conditions: earthquakes, rainfall, adjacent structures, future works loads, etc.
- Tunnel position regards the slope: should the tunnel be located at the bottom of the slope with high stress levels, this can result in greater displacements and loads on the support (Koizumi et al., 2010).
- Shape and dimensions of the tunnel: the smaller the tunnel section, the lower the impact (Causse et al., 2015b), which is also affected by its shape and geometry.
- Functional configuration (Vlachopoulos & Vazaios, 2015): twin tunnels, designed in most cases for roads and railways, impose more complex tensional configurations and overlapping effects.
- Construction method and its consequent deconfinement: adopted equipment, number of excavations and support stages, delay in support installation, etc. (Causse et al., 2015a).
- Support properties: support system, thickness, stiffness, etc.

In summary, during the planning and design of tunnels near slopes it is required to study the conditions of the ground excavation, to verify whether it is needed to move the tunnel away from the slope or potential slip surface and/or design additional rock support to deal with the specifics of the tunnel-slope interaction.

## 3 CALCULATION HYPOTHESIS

Based on numerical simulations conducted with Plaxis 2D software, the purpose of this research is to show how the construction of a circular tunnel modifies both its primary support requirements and the stability conditions of a slope close to the cavity. The main variables considered are as follows:

- Diameter of the tunnel ( $D$ ) = 10 m.
- Height of the slope ( $H$ ) = 40 and 80 m ( $4D$  and  $8D$ ).
- Tunnel-slope distance ( $d$ ) = 5 to 50 m ( $0.5D$ ,  $1D$ ,  $1.5D$ ,  $2D$ , and  $5D$ )
- Geological Stress Index of the rock mass ( $GSI$ ) = 20, 25, 30, and 40.

Competent rock masses, also known as those with low fracturing and high strength, can be bored while keeping an elastic regime, in which the tunnel-slope interaction becomes more an issue of block kinematics than a stress interaction analysis. Because of that, medium to low qualities of the rock mass have been selected in this study ( $GSI$  from 20 to 40).

The geometry of the numerical models (see Figure 1) was defined as a function of parameters ( $D$ ), ( $H$ ) and ( $d$ ). For all calculations, a slope of 1V:1H ( $45^\circ$  inclination) was considered. In addition, variable ( $d$ ) has always been set from the midpoint of the slope. Models between 4000 and 12000 elements have been obtained, with a refined mesh near the tunnel and slope in all situations (dark-gray areas shown in Figure 1).

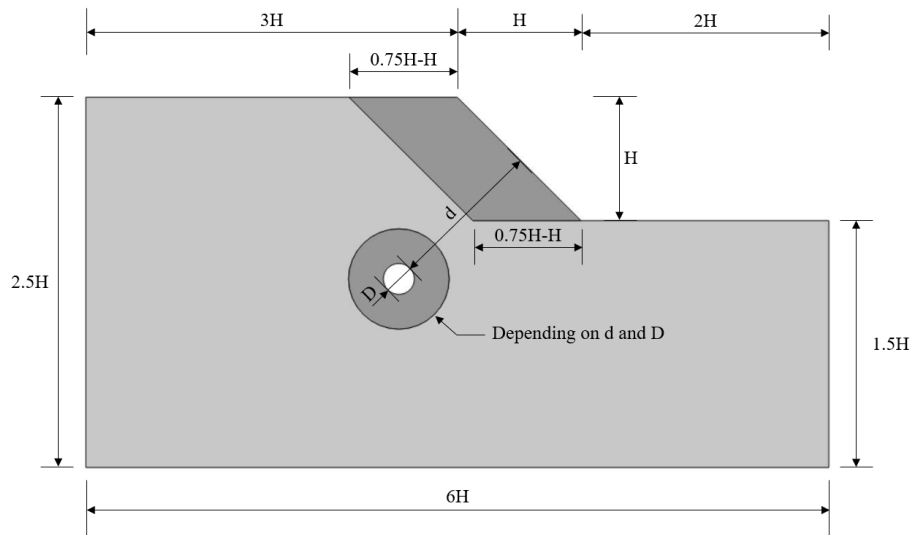


Figure 1. Geometry of the numerical models.

Assuming the Hoek-Brown failure criterion, different rock mass properties have been defined depending on the ( $GSI$ ) value (see Table 1). No water table and a coefficient of earth pressure at rest ( $k_0$ ) equal to 1 were also established. The primary support was considered as a ring of concrete, which thickness ( $e$ ) also varies with the parameter ( $GSI$ ). The values of ( $e$ ) included in Table 1 have been previously verified, checking that the results from the axial force-bending moment interaction could be supported by the concrete lining in every model. Concrete properties for 1 and 28 days have been estimated from concrete uniaxial compressive strengths of 12.7 and 30 MPa, respectively.

Because the analysis was performed in 2D (plane strain), the construction of the tunnel had to be simulated with an intermediate phase of deconfinement prior to the support installation. Following the formulation from Carranza-Torres & Fairhurst (2000), a sensitivity study was carried out assuming full-face excavation. As a result, a deconfinement value of 50% was considered accurate enough to reproduce the general behavior of all the numerical models to be calculated.

Table 1. Parameters depending on the  $GSI$  value: rock mass properties & primary support thickness.

$GSI$	$m_i$ <sup>(1)</sup>	$\sigma_{ci}$ [MPa] <sup>(1)</sup>	$D^*$ <sup>(1)</sup>	$\gamma$ [kN/m <sup>3</sup> ] <sup>(2)</sup>	$E$ [MPa] <sup>(3)</sup>	$\nu$ <sup>(2)</sup>	$e$ [cm]
20	10	20	0	25	795.3	0.3	70
25	10	20	0	25	1060.5	0.3	60
30	10	20	0	25	1414.2	0.3	50
40	10	20	0	25	2514.9	0.3	35

<sup>(1)</sup> Intact rock constant ( $m_i$ ), uniaxial compressive strength ( $\sigma_{ci}$ ), and disturbance factor ( $D^*$ ) from Hoek-Brown failure criterion.

<sup>(2)</sup> Specific weight ( $\gamma$ ) and Poisson's coefficient ( $\nu$ ).

<sup>(3)</sup> Elastic modulus of the rock mass ( $E$ ) obtained using the formulation from Hoek et al. (2002).

## 4 RESULTS

### 4.1 Tunnel deformations

As could be expected, the results obtained show that the lower the index ( $GSI$ ) and the higher the slope height ( $H$ ), the greater the tunnel deformations. Assuming ( $H$ ) = 80 m, the most representative deformations are included in Figure 2, as a function of index ( $GSI$ ) and distance ( $d$ ). In that figure, it can be observed that both the tunnel crown and the tunnel invert tend to close inward. The deeper the tunnel, the more it closes. However, the tunnel sidewalls are where the tunnel-slope interaction effects are best identified. As shown in Figure 2b, the shorter the distance to the slope, the greater the sidewalls displacements, tending to open the tunnel towards the slope instead of closing it.

It should be noticed in Figure 2b that the maximum deformations of the sidewalls do not occur for the shallowest calculation scenario, due to the influence of the tunnel on the stability conditions of the slope. As represented in the following paragraphs, when the tunnel affects the potential slip surface of the slope the tunnel deformations tend to increase, as well as the axial forces and the bending moments for the primary support, while the safety factor of the slope tend to decrease.

Another aspect that should be mentioned is the non-symmetry of the tunnel deformations. Due to the modelling of the slope, the principal stresses in the area where the tunnel is located are not the vertical and horizontal directions. Parameter ( $k_{\theta}$ ) = 1 is only verified near the model contours. As a result, even for the deepest calculation scenarios the tunnel deformations are slightly rotated.

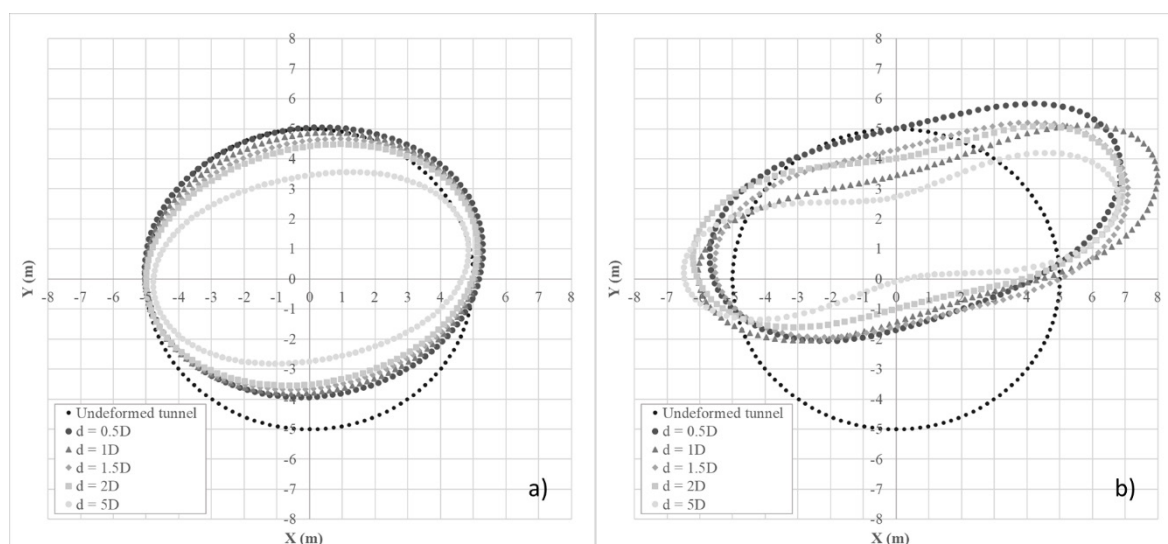


Figure 2. Deformed tunnel with primary support (1 day) and  $H=80m$ . a)  $GSI=40$ ; b)  $GSI=20$ .  
Scale: 1 m of deformed tunnel = 1 mm of real deformation.

### 4.2 Slip surface

Due to the tunnel-slope interaction, the potential slip surface of the slope changes depending on the position of the tunnel (see Figure 3). For a tunnel-slope distance larger than 20 m ( $d=2D$ ), the results show almost no influence in the potential shape of the rupture. Instead, shorter distances ( $d=0.5D$  and  $d=1D$ ) confirm notable changes in its development. Calculations for 15 m of distance ( $d=1.5D$ ) seem to be an intermediate situation between the two previous situations.

### 4.3 Axial forces and bending moments

As shown in Figure 4a, maximum axial forces on the primary support (1 day) increase with the tunnel depth, with minor affections due to the tunnel-slope interaction. These results are consistent with the greater rock cover over the tunnel crown as the tunnel moves away from the slope. Instead, bending

moments follow a different pattern for the same range of tunnel-slope distances analyzed (see Figure 4b), showing maximum values in the shallowest calculation scenarios affected by the potential slip surface of the slope. As a result, the design of the primary support for those situations is governed by the eccentricity of the loads due to the tunnel-slope interaction. It is important to highlight that the maximum bending moments are not corresponding to the minimum cover but depending on the position of the tunnel regards the potential slip surface.

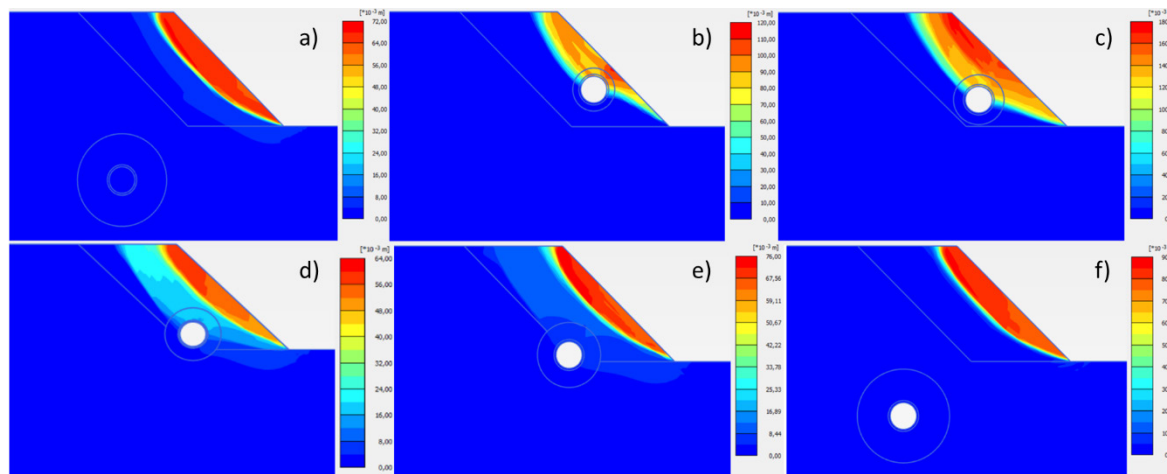


Figure 3. Failure surface after *FOS* calculations. Total displacements with primary support (1 day),  $D=10m$ ,  $H=40m$ , and  $GSI=20$ . a) Slope without tunnel; b)  $d=0.5D$ ; c)  $d=1D$ ; d)  $d=1.5D$ ; e)  $d=2D$ ; f)  $d=5D$ .

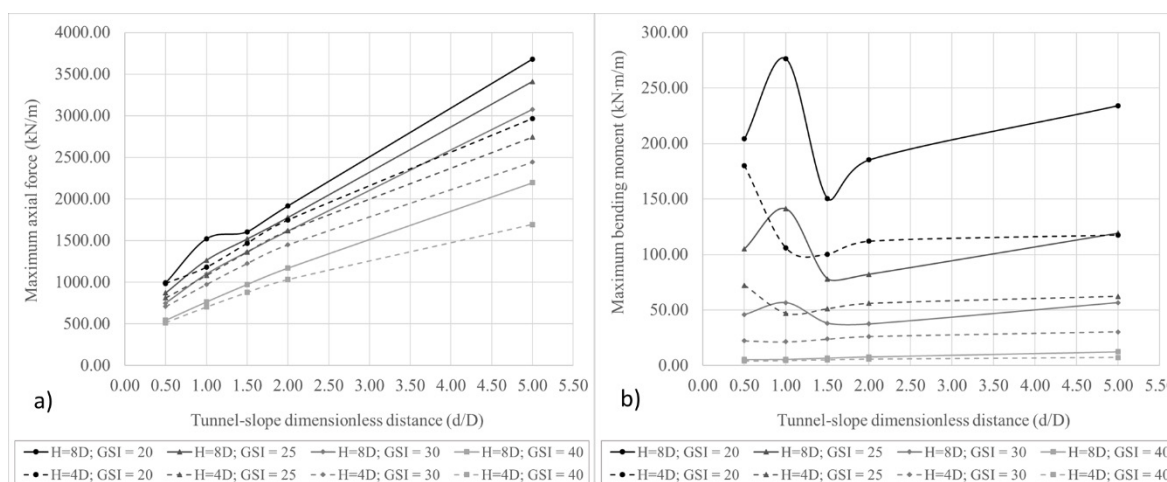


Figure 4. Primary support (1 day) results. a) Axial forces; b) Bending moments.

#### 4.4 Factor of safety (*FOS*)

Table 2 includes the factor of safety (*FOS*) results from this research, as a function of parameters (*GSI*), (*d*) and (*H*). These values show that the deconfinement phase is the one with the lowest safety factor, barely above 1 for the most unfavorable scenario ( $FOS=1.06$  when  $D=10m$ ,  $GSI=20$ ,  $d=0.5D$ , and  $H=8D$ ). The safety of the slope tends to increase after the primary support installation, reaching values close to the safety factor of the slope without the tunnel.

When the tunnel is far enough from the slope, the (*FOS*) results are not affected by the tunnel construction. For a slope height of 80 m ( $H=8D$ ) and a tunnel-slope distance of 50 m ( $d=5D$ ), the safety values obtained in all the calculation phases are the same. In the case of ( $H=40m$  ( $H=4D$ ), the same phenomenon at a shorter tunnel-slope distance is observed, starting from ( $d=20m$  ( $d=2D$ ).

Table 2. Factor of safety values for  $D=10m$ , depending on parameters  $GSI$ ,  $d$ , and  $H$ .

Staged construction	$GSI$	$d=0.5D$		$d=1D$		$d=1.5D$		$d=2D$		$d=5D$	
		$H=4D$	$H=8D$	$H=4D$	$H=8D$	$H=4D$	$H=8D$	$H=4D$	$H=8D$	$H=4D$	$H=8D$
Slope without tunnel	20	1.55	1.27	1.55	1.27	1.55	1.27	1.55	1.27	1.55	1.27
	25	1.76	1.42	1.76	1.42	1.76	1.42	1.76	1.42	1.76	1.42
	30	1.97	1.57	1.97	1.57	1.97	1.57	1.97	1.57	1.97	1.57
	40	2.45	1.88	2.45	1.88	2.45	1.88	2.45	1.88	2.45	1.88
Tunnel with 50% deconfinement	20	1.12	1.06	1.29	1.08	1.50	1.12	1.55	1.19	1.55	1.27
	25	1.28	1.16	1.43	1.21	1.66	1.25	1.76	1.31	1.76	1.42
	30	1.45	1.32	1.62	1.33	1.82	1.38	1.97	1.43	1.97	1.57
	40	1.94	1.64	2.03	1.68	2.20	1.69	2.38	1.71	2.45	1.88
Concrete lining (1 day)	20	1.29	1.14	1.42	1.12	1.55	1.16	1.55	1.22	1.55	1.27
	25	1.40	1.27	1.53	1.21	1.73	1.27	1.76	1.32	1.76	1.42
	30	1.53	1.40	1.66	1.34	1.84	1.38	1.97	1.44	1.97	1.57
	40	1.95	1.78	2.03	1.68	2.20	1.69	2.38	1.71	2.45	1.88
Concrete lining (28 days)	20	1.40	1.19	1.52	1.16	1.55	1.21	1.55	1.25	1.55	1.27
	25	1.48	1.30	1.62	1.24	1.76	1.30	1.76	1.36	1.76	1.42
	30	1.60	1.41	1.73	1.36	1.96	1.40	1.97	1.46	1.97	1.57
	40	2.02	1.82	2.05	1.69	2.27	1.70	2.45	1.73	2.45	1.88

## 5 CONCLUSIONS

Numerical simulations carried out in this research confirm the expected tunnel-slope interaction effects. Slope stability is modified when the tunnel is close enough to its potential slip surface, compromising the safety of both the slope and the tunnel itself. Tunnel deformations and bending moments are the most affected by the tunnel-slope interaction, requiring additional support to face this phenomenon without losing its functionality.

To avoid tunnel-slope interaction in weak rock masses, more than 2 diameters of distance ( $d=2D$ ) should be ensured, although the main recommendation of this research is to carry out specific studies unless elastic behavior in competent rock masses is proven. The greater the ( $H/D$ ) relation, the larger the relative distance ( $d/D$ ) has to be for the tunnel to not affect the stability of the slope.

## REFERENCES

- Carranza-Torres, C., Fairhurst, C. 2000. Application of the Convergence-Confinement Method of Tunnel Design to Rock Masses that Satisfy the Hoek-Brown Failure Criterion. *Tunnelling and Underground Space Technology*, Vol 15, N 2, pp. 187-213, 2000.
- Causse, L., Cojean, R. Fleurisson, J.A. 2015a. Interaction between tunnel and unstable slope – Influence of time dependent behavior of a tunnel excavation in a deep-seated gravitational slope deformation. *Tunnelling and Underground Space Technology*. Volume 50, August 2015, Pages 270-281.
- Causse, L., Cojean, R. Fleurisson, J.A. 2015b. Interactions Between Tunnels and Unstable Slopes: Role of Excavation. <https://hal.archives-ouvertes.fr/hal-01112269>. Feb 2015.
- Hoek, E., Carranza-Torres, C., Corkum, B. 2002. Hoek-Brown failure criterion – 2002 Edition. *Proc. NARMS-TAC Conference, Toronto, 2002*, 1, 267-273
- Koizumi, Y., J. Lee, K. Date, Y. Yokota, T. Yamamoto, K. Fujisawa. 2010. Numerical analysis of landslide behavior induced by tunnel excavation. *Rock Mechanics in Civil and Environmental Engineering – Zhao, Labiouse, Dudt & Mathier (eds)*.
- Sanchez, S., Garrido C. 2022. Interacción entre túneles y laderas. De causa de inestabilidad a técnica de remediación. *X Simposio Nacional sobre Taludes y Laderas Inestables*. Granada, septiembre 2022.
- Vlachopoulos N. & Vazaios I. 2015. Case Study: The Influence of Tunnelling on Slope Stability. *Conference paper. GeoQuebec 2015*.
- Wang, T.T., 2010. Characterizing crack patterns on tunnel linings associated with shear deformation induced by instability of neighboring slopes. *Eng. Geol.* 115, 80–95.